J. Plasma Physics (2005), *vol.* 71, *part* 3, *pp.* 359–366. © 2005 Cambridge University Press
doi:10.1017/S0022377804003319 Printed in the United Kingdom

Second harmonic generation in a laser channel

A. UPADHYAY[1] and V. K. TRIPATHI[2]

[1]Laser Plasma Division, Center for Advanced Technology, Indore 452 013, India
(ajitup@cat.ernet.in)
[2]Department of Physics, Indian Institute of Technology, New Delhi 110 016, India

(Received August 2004, revised October 2004 and accepted October 2004)

Abstract. An intense laser beam guided through a low-density plasma channel produces second harmonic emission that leaks out in the high-density outer region, propagating in a low-angle hollow cone with respect to channel axis. For a channel with interior density $0.25n_{cr}$, outer region density $0.64n_{cr}$ (n_{cr} being the critical density), laser wavelength 1 μ and channel radius $\sim$5 μm, the angle θ of the cone $\sim$19°. The second harmonic power shows an oscillatory behavior with the density of the channel. It peaks at certain densities of the plasma channel. The heights of the peaks of second harmonic power are higher at greater densities.

1. Introduction

Harmonic generation of high-power lasers in plasma is an important nonlinear process observed in experiments [1, 2]. It acts as a valuable diagnostic in short pulse laser–plasma interaction and has received considerable attention in recent years. The harmonic emission takes place when the fundamental light is reflected in a steep density profile off the critical density surface [3–5]. Harmonic generation in under-dense plasmas is characterized by two important features. First, the momentum of the nth harmonic photon is larger than n times the momentum of fundamental photon, hence, the process is non-resonant. Second, the power density of nth harmonic goes as the nth power of the fundamental wave power density. Engers et al. [6] have reported second harmonic generation in plasmas produced by an intense ultra short laser pulse. A comprehensive analysis of harmonic generation by intense lasers has been given by Esarey et al. [7]. Zepf et al. [8] have investigated the generation of high harmonics from the interaction of ultra short intense laser pulses with solid targets. They have demonstrated that the conversion efficiency depends strongly on the density scale length. Mori et al. [9], Wilks et al. [10] and Rax and Fisch [11, 12] have investigated the relativistic odd harmonic content of an intense laser propagating in under-dense plasma and over-dense plasma. It is observed that, in the absence of damping or density gradients, the harmonic amplitude oscillates between zero and twice the steady-state value. Liu and Tripathi [13] have studied the second harmonic generation of Raman backscattered light [14] in a plasma channel. The intense short pulse laser produces a wave via Raman backscattering. In the region of the wake, the plasma shrinks in size, and forms a narrow plasma channel. The channel breaks into bubbles via oscillating two-stream instability on a picosecond time scale. The Raman backscattered wave propagating

https://doi.org/10.1017/S0022377804003319 Published online by Cambridge University Press

through the channel of bubbles generates a second harmonic, observed at oblique angles.

Stamper et al. [15] have observed second harmonic emission from filamentary structures at densities $n/n_{cr} \sim 0.03$–0.10. They showed that second harmonic emission may be due to either a reflected wave or stimulated Brillouin scattering within the filament. Young et al. [16] have observed that the second harmonic emission is spatially correlated with the density perturbations, but is not observed for the entire length of filament. According to them, the chief source of second harmonic emission is filamentary focus rather than emission along the length of filament. Brandi et al. [17], in their study of laser interaction with inhomogeneous plasma, have reported that the second harmonic power is independent of plasma density in the low-density limit whereas the power generated is proportional to square of laser intensity. Malka et al. [18] have observed second harmonic emission that is phase modulated by a co-propagating relativistic electron plasma wave produced by forward Raman scattering. From the observation of filamentary shaped images, they infer that relativistic and/or ponderomotive self-focusing may occur. Meyer and Zhu [19] have reported the theory of second harmonic emission from the tight focus of a laser arising from filamentation instability (focal radius $\sim\lambda_0$). None of the above-mentioned papers deal with second harmonic emission from a plasma slab and its leakage into the outside region. An intense laser beam guided through a low-density plasma channel [20] produces second harmonic emission that leaks out in the high-density outer region, propagating in a low-angle hollow cone with respect to channel axis. The channel helps in achieving higher efficiencies of harmonic generation by providing higher fundamental wave power density over a long length.

In this paper we study the generation of the second harmonic emission of laser radiation in a pre-formed low-density plasma channel. In Sec. 2, we derive the second harmonic nonlinear current density. In Sec. 3, the second harmonic power is calculated. Section 4 contains discussions.

2. Second harmonic nonlinear current density

Consider the propagation of a laser along $\hat{z}$ through a plasma channel. We consider the laser field amplitude such that the diffraction divergence is exactly balanced by self-focusing and the laser is self-guided. The density profile $n_0(x)$ of the channel is

$$n_0(x) = \begin{cases} n_{01} & |x| < a, \\ n_0 & |x| > a, \end{cases} \tag{1}$$

and $n_{01} < n_0$. The laser field can be taken as

$$\mathbf{E} = \hat{y} A_0 e^{-i(\omega_0 t - k_0 z)}.$$

We only consider the fundamental radial eigenmode of the laser. The equation governing A_0 in different regions are

$$\begin{aligned} &\frac{\partial^2 A_0}{\partial x^2} + k_{0\perp}^2 A_0 = 0 \quad |x| < a \\ &\frac{\partial^2 A_0}{\partial x^2} - \alpha_0^2 A_0 = 0 \quad |x| > a, \end{aligned} \tag{2}$$

https://doi.org/10.1017/S0022377804003319 Published online by Cambridge University Press

where

$$k_{0\perp}^2 = \frac{\omega_0^2 - \omega_{\rm p1}^2}{c^2} - k_{0z}^2, \quad \omega_{\rm p1} = (4\pi n_{01} e^2/m)^{1/2},$$

$$\alpha_0^2 = k_{0z}^2 - \frac{\omega_0^2 - \omega_{\rm p2}^2}{c^2}, \quad \omega_{\rm p2} = (4\pi n_0 e^2/m)^{1/2}$$

and gives symmetric solutions for A_0:

$$A_0 = \begin{cases} A_{01}\, e^{-\alpha_0 x} & x > a, \\ A_{00}\, \cos k_{0\perp} x & |x| < a, \\ A_{01}\, e^{\alpha_0 x} & x < -a. \end{cases} \tag{3}$$

Continuity of the tangential component of the electric and magnetic field at $x = \pm a$ gives the dispersion relation for the pump laser

$$\tan(k_{0\perp} a) = \alpha_0 / k_{0\perp}. \tag{4}$$

The laser imparts oscillatory velocity to electrons

$$\mathbf{v}_0 = \frac{e\mathbf{E}_0}{mi\omega_0}$$

and exerts a $\mathbf{v}_0 \times \mathbf{B}_0$ force on electrons

$$\mathbf{F}_{2\omega_0} = -\frac{ek_{0z}}{2\omega_0} v_0 E_0 \hat{z} + i\frac{ev_0}{2\omega_0}\frac{\partial E_0}{\partial x}\hat{x}.$$

This force produces oscillatory velocity and density fluctuations at $2\omega_0$, causing a nonlinear current density at $2\omega_0$.

$$\mathbf{v}_{2\omega_0}^{\rm NL} = -\frac{e^2}{4\omega_0^3 m^2}\left[E_0^2 k_{0z}\hat{z} + iE_0\frac{\partial E_0}{\partial x}\hat{x}\right] \tag{5}$$

$$\mathbf{J}_{2\omega_0}^{\rm NL} = -n_0 e \mathbf{v}_{2\omega_0}. \tag{6}$$

The wave equation for the second harmonic is

$$-\nabla(\nabla\cdot\mathbf{E}_2) + \nabla^2\mathbf{E}_2 + \frac{4\omega_0^2 - \omega_{\rm p}^2}{c^2}\mathbf{E}_2 = -\frac{8\pi i\omega_0}{c^2}\mathbf{J}_{2\omega_0}^{\rm NL} \tag{7}$$

taking ∇ of this equation

$$\nabla\cdot\mathbf{E}_2 = -\frac{8\pi i\omega_0}{4\omega_0^2 - \omega_{\rm p}^2}\nabla\cdot\mathbf{J}_{2\omega_0}^{\rm NL}. \tag{8}$$

Using (8) in (7), we get

$$\nabla^2\mathbf{E}_2 + \frac{4\omega_0^2 - \omega_{\rm p}^2}{c^2}\mathbf{E}_2 = -\frac{8\pi i\omega_0}{c^2}\mathbf{J}_{2\omega_0}^{\rm NL} + \nabla\left(-\frac{8\pi i\omega_0}{4\omega_0^2 - \omega_{\rm p}^2}\nabla\cdot\mathbf{J}_{2\omega_0}^{\rm NL}\right). \tag{9}$$

We solve (9) for three different regions, $|x| < a$, $x > a$ and $x < -a$.

Region I: $|x| < a$

We write the $\hat{z}$ component of the wave equation

$$\frac{\partial^2 E_{2z}}{\partial x^2} + k_{2x}^2 E_{2z} = i\frac{\omega_{\rm p1}^2 k_{0z}}{4\omega_0}\frac{k_{2x}^2}{4\omega_0^2 - \omega_{\rm p1}^2}|v_0|A_0(1 + e^{2ik_{0\perp}x} + e^{-2ik_{0\perp}x}), \tag{10}$$

https://doi.org/10.1017/S0022377804003319 Published online by Cambridge University Press

where $k_{2x}^2 = (4\omega_0^2 - \omega_{\rm p1}^2 - 4k_{0z}^2c^2)/c^2$. The solution of (10) is written as

$$E_{2z\rm I} = D_1 e^{ik_{2x}x} + D_2 e^{-ik_{2x}x} + i\frac{\omega_{\rm p1}^2 k_{0z}}{4\omega_0}\frac{k_{2x}^2}{4\omega_0^2 - \omega_{\rm p1}^2}|v_0|A_0\left[\frac{e^{ik_{2x}x} + e^{-ik_{2x}x}}{k_{2x}^2 - 4k_{0\perp}^2}\right] \quad (11)$$

where D_1 and D_2 are coefficients. Here we have neglected the terms only contributing towards the space charge oscillations. Using (8) and (11), we write the $\hat{x}$ component of the field as

$$E_{2x\rm I} = \int -2ik_{0z}E_{2z\rm I}\,dx - \frac{16\pi\omega_0}{4\omega_0^2 - \omega_{\rm p1}^2}n_0^0 e\int \mathbf{k}_0\cdot\mathbf{v}_{2\omega_0}\,dx \quad (12)$$

or

$$\begin{aligned} E_{2x\rm I} = &-\frac{2k_{0z}}{k_{2x}}(D_1 e^{ik_{2x}x} - D_2 e^{-ik_{2x}x}) \\ &- i\frac{\omega_{\rm p1}^2 k_{0z}}{4\omega_0}\frac{k_{2x}^2}{4\omega_0^2 - \omega_{\rm p1}^2}\frac{k_{0z}}{k_{0\perp}}|v_0|A_0\left[\frac{e^{ik_{2x}x} + e^{-ik_{2x}x}}{k_{2x}^2 - 4k_{0\perp}^2}\right] \\ &+ \frac{\omega_{\rm p1}^2 k_{0z}}{2\omega_0}\frac{1}{4\omega_0^2 - \omega_{\rm p1}^2}|v_0|A_0\left(\frac{k_{0z}}{k_{0\perp}}\sin(2k_{0\perp}x) - i\frac{k_{0\perp}}{2k_{0z}}\cos(2k_{0\perp}x)\right). \end{aligned} \quad (13)$$

Region II: $x > a$

We write the wave equation for region II. Region III is symmetric to region II, so does not need to be solved:

$$\frac{\partial^2 E_{2z\rm II}}{\partial x^2} + k_{2x}'^2 E_{2z\rm II} = i\frac{\omega_{\rm p2}^2 k_{0z}}{2\omega_0}\frac{k_{2x}'^2}{4\omega_0^2 - \omega_{\rm p2}^2}|v_0|A_0 e^{-2\alpha_0 x}. \quad (14)$$

The solution to (14) is written as

$$E_{2z\rm II} = D_3 e^{-ik_{2x}'x} + i\frac{\omega_{\rm p2}^2 k_{0z}}{2\omega_0}\frac{k_{2x}'^2}{4\omega_0^2 - \omega_{\rm p2}^2}|v_0|A_0\left[\frac{e^{-2\alpha_0 x}}{k_{2x}'^2 + 4\alpha_0^2}\right]. \quad (15)$$

Following the same treatment as in region I for the $\hat{x}$ component of electric field, we get

$$\begin{aligned} E_{2x\rm II} = &D_3 e^{-ik_{2x}'x}\cdot\frac{2k_{0z}}{k_{2x}'} - \frac{\omega_{\rm p2}^2 k_{0z}}{2\omega_0}\frac{k_{2x}'^2}{4\omega_0^2 - \omega_{\rm p2}^2}\frac{k_{0z}}{\alpha_0}|v_0|A_0\left[\frac{e^{-2\alpha_0 x}}{k_{2x}'^2 + 4\alpha_0^2}\right] \\ &+ \frac{\omega_{\rm p2}^2 k_{0z}}{2\omega_0}\frac{|v_0|A_0}{4\omega_0^2 - \omega_{\rm p2}^2}\left(\frac{k_{0z}}{k_{0\perp}}\sin(2k_{0\perp}x) - i\frac{k_{0\perp}}{2k_{0z}}\cos(2k_{0\perp}x)\right), \end{aligned} \quad (16)$$

where D_3 is the coefficient to be evaluated. We have the continuity condition

$$E_{2z\rm I}|_{x=a} = E_{2z\rm II}|_{x=a} \quad \text{and} \quad \varepsilon_{2\rm I}E_{2x\rm I}|_{x=a} = \varepsilon_{2\rm II}E_{2x\rm II}|_{x=a}. \quad (17)$$

Applying (17) at $x = -a$ gives $D_1 = D_2$. Using (11), (13), (15) and (16) in (17) and solving for D_3, we get

$$D_3 = \frac{p_1 + iq_1}{p_2 + iq_2}A_0,$$

https://doi.org/10.1017/S0022377804003319 Published online by Cambridge University Press

where

$$p_1 = \frac{8K'k_{0z}}{\beta k_{2x}}\sin(k_{2x}a)e^{-2\alpha_0 a} + \left(\frac{2\Omega K'}{k_{2x}'^2} - \frac{4K}{k_{2x}^2}\right)\frac{k_{0z}}{k_{0\perp}}\cos(k_{2x}a)\sin(2k_{0\perp}a)$$

$$+ \frac{4Kk_{0z}}{\gamma k_{0\perp}}\cos(k_{2x}a)\cos(2k_{0\perp}a) - \frac{4\Omega K'}{\beta}\frac{k_{0z}}{\alpha_0}\cos(k_{2x}a)e^{-2\alpha_0 a},$$

$$q_1 = \left(\frac{2K}{k_{2x}^2} - \frac{2\Omega K'}{k_{2x}'^2}\right)\frac{k_{0\perp}}{k_{0z}}\cos(k_{2x}a)\cos(2k_{0\perp}a) - \frac{8Kk_{0z}}{\gamma k_{2x}}\sin(2k_{0\perp}a),$$

$$p_2 = \frac{4k_{0z}}{k_{2x}}\sin(k_{2x}a)\sin(k'_{2x}a) - \frac{4\Omega k_{0z}}{k'_{2x}}\cos(k_{2x}a)\cos(k'_{2x}a), \tag{18}$$

$$q_2 = \frac{4k_{0z}}{k_{2x}}\sin(k_{2x}a)\cos(k'_{2x}a) + \frac{4\Omega k_{0z}}{k'_{2x}}\cos(k_{2x}a)\sin(k'_{2x}a),$$

$$K = \frac{\omega_{\mathrm{p1}}^2 k_{0z}}{4\omega_0}\frac{k_{2x}^2}{4\omega_0^2 - \omega_{\mathrm{p1}}^2}|v_0|, \quad K' = \frac{\omega_{\mathrm{p2}}^2 k_{0z}}{4\omega_0}\frac{k_{2x}'^2}{4\omega_0^2 - \omega_{\mathrm{p2}}^2}|v_0|,$$

$$\Omega = \frac{4\omega_0^2 - \omega_{\mathrm{p2}}^2}{4\omega_0^2 - \omega_{\mathrm{p1}}^2}, \quad \beta = k_{2x}'^2 + 4\alpha_0^2,$$

and $\gamma = k_{2x}^2 - 4k_{0\perp}^2$.

3. Second harmonic power

The field amplitude of second harmonic $E_{2\mathrm{II}}$ in region II is given by

$$|E_{2\mathrm{II}}|^2 = E_{2x\mathrm{II}}^2 + E_{2z\mathrm{II}}^2 = D_3^2\left[1 + \frac{4k_{0z}^2}{k_{2x}'^2}\right]. \tag{19}$$

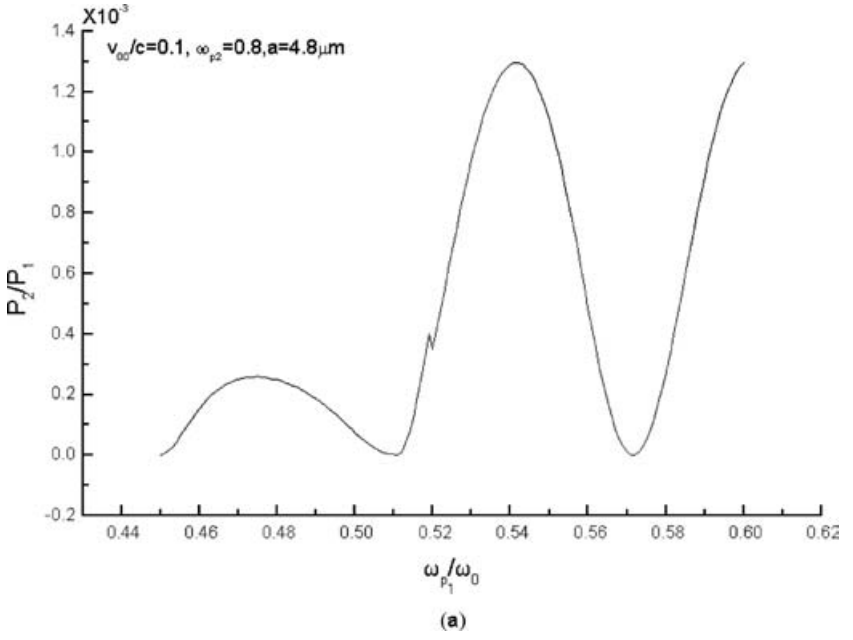
The total second harmonic power radiated in a conical annular ring at angle θ from a channel of length L would be

$$P_2 = \frac{c}{8\pi}|E_{2\mathrm{II}}|^2[(L\sin\theta a)^2 + 2L\tan(\theta)/a], \tag{20}$$

where $\theta = \tan^{-1}(k'_{2x}/k_{2z})$ is the angle of second harmonic emission. We calculate second harmonic power P_2 for the following parameters: $\lambda \sim 1$ μm, $L = 150$ μm, $\omega_{\mathrm{p2}}/\omega_0 = 0.8$, $\omega_{\mathrm{p1}}/\omega_0 = 0.45$–$0.6$, $v_0/c = 0.1$ and $a = 4.8, 9.6$ μm. The relative second harmonic power ($\sim P_2/P_1$) versus $\omega_{\mathrm{p1}}/\omega_0$ is plotted in Fig. 1. The second harmonic power shows an oscillatory behavior with the density of the plasma channel. It peaks at certain densities of plasma channel and the peak value increases with the increasing density of the channel. An increase in the channel width increases the number of densities at which the peaks occur. The maximum value of the second harmonic power at these densities also increases with increasing channel radius. It is also observed that the second harmonic power increases linearly with increasing length of the plasma channel. We have

$$k_{0z}^2 = \frac{\omega_0^2 - \omega_{\mathrm{p1}}^2}{c^2} - k_{0\perp}^2, \tag{21}$$

https://doi.org/10.1017/S0022377804003319 Published online by Cambridge University Press



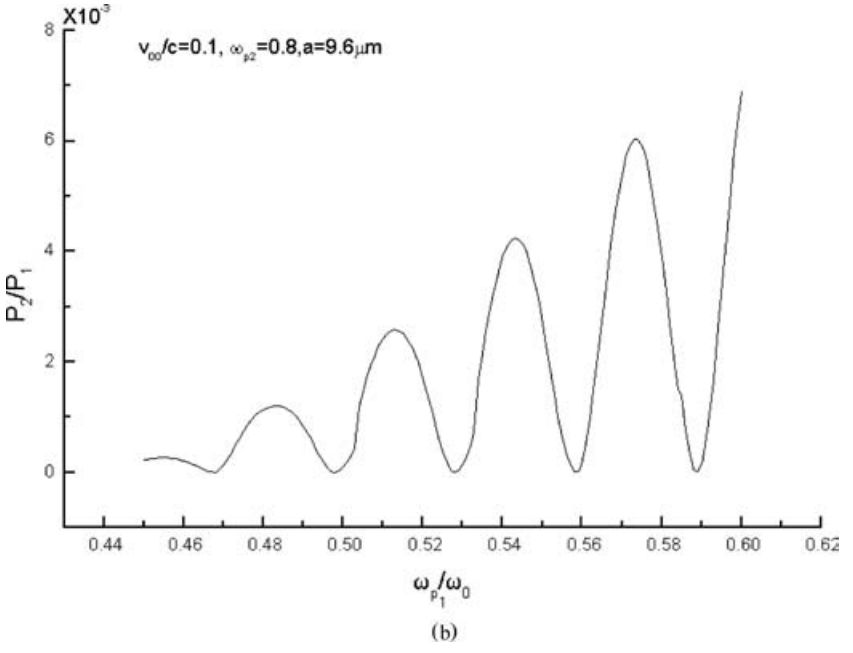


Figure 1. (a) Second harmonic conversion efficiency ($\sim P_2/P_1$) versus density of plasma channel ($\omega_{\rm p1}/\omega_0$) for channel radius $a = 4.8$ μm. (b) Second harmonic conversion efficiency ($\sim P_2/P_1$) versus density of plasma channel ($\omega_{\rm p1}/\omega_0$) for channel radius $a = 9.6$ μm.

https://doi.org/10.1017/S0022377804003319 Published online by Cambridge University Press

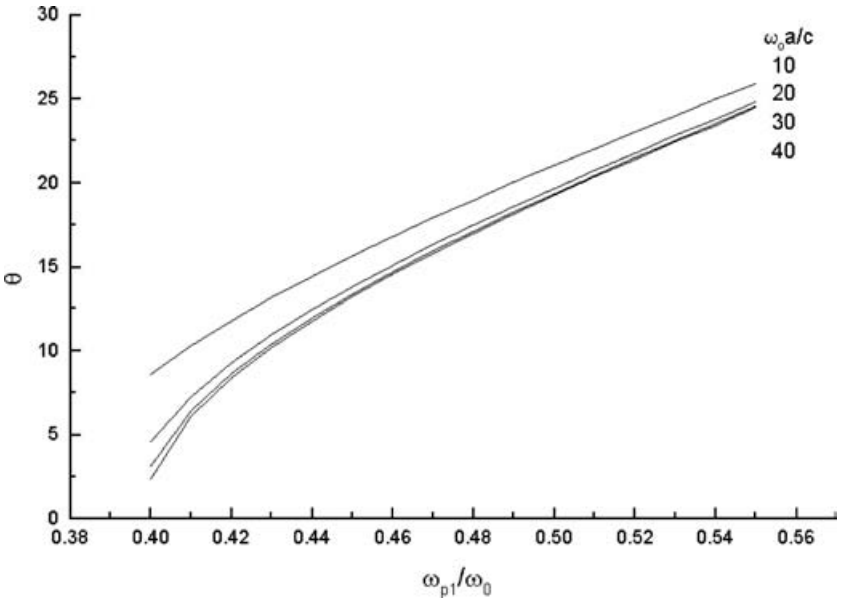


Figure 2. Angle of second harmonic emission (θ) versus density of the plasma channel ($\omega_{\mathrm{p1}}/\omega_0$).

where $k_{0\perp}$ is given by (4) and

$$k_{2x}^2 = \frac{4\omega_0^2 - \omega_{\mathrm{p1}}^2}{c^2} - 4k_{0z}^2, \tag{22}$$

$$k_{2x}'^2 = \frac{4\omega_0^2 - \omega_{\mathrm{p2}}^2}{c^2} - 4k_{0z}^2, \tag{23}$$

$$k_{2z} = 2k_{0z}. \tag{24}$$

Using (23) and (24) with (4) and (21), k_{0z} and θ, the angle at which the second harmonic emission takes place, are obtained. The angle θ versus $\omega_{\mathrm{p1}}/\omega_0$ is plotted in Fig. 2 for $\omega_{\mathrm{p2}}/\omega_0 = 0.8$, $\omega_{0a}/c = 10$–40 and $\omega_{\mathrm{p1}}/\omega_0 = 0.3$–$0.55$. It is observed that θ increases linearly with ω_{p1}, the density of plasma channel. At slightly lower densities ($\omega_{\mathrm{p1}}/\omega_0 \sim 0.4$), the increase in the angle of second harmonic emission greater with increasing ω_{p1}.

4. Discussion

A laser guided in a low-density plasma channel appears to produce second harmonic emission at reasonably high efficiency. The second harmonic power leaks out into the higher density outer region at a small angle to channel axis. The nonlinearity is caused by the ponderomotive force. The harmonic power shows oscillatory behavior with the density of the channel. The heights of the peaks are stronger at higher densities. The second harmonic power peaks more frequently and the maximum value of peak increases linearly with increasing channel radius. It increases linearly with the length of the channel. The periodic variation of second harmonic amplitude with channel density appears due to the fact that the second harmonic field depends on $k_{0\perp}$ through sine and cosine functions and that $k_{0\perp}$depends on channel density. The density of channel, in our analysis, is restricted to $\omega_{\mathrm{p1}} < \omega_{\mathrm{p2}}$ so as to enable the

https://doi.org/10.1017/S0022377804003319 Published online by Cambridge University Press

guiding of the laser into the channel. If one takes $\omega_{p1} = \omega_{p2}$, no laser guiding would take place and the above analysis would not be valid for such a case. Mori et al. [9] have observed similar features in their computer simulation of third harmonic generation. They have reported the variation of third harmonic power for $v_0/c = 0.2$–1.0, $\omega_p/\omega_0 = 0.01$–0.20, the density profile width $0.1c/\omega_{p0}$–$300c/\omega_{p0}$ and have observed the oscillatory behavior of third harmonic power with the density of the plasma. Although the theory of third harmonic generation is altogether different, the results observed are nevertheless similar. Our treatment is only valid for a self-guided laser and not for a converging beam.

References

[1] Castillo-Herrera, C. I. and Johnston, T. W. 1993 Incoherent harmonic emission from strong electromagnetic waves in plasmas. *IEEE Trans. Plasma Sci.* **21**, 120.

[2] Matsumoto, M. and Tanaka, K. 1995 Quasi-phase-matched second-harmonic generation by backward propagating interaction. *IEEE J. Quantum Electron.* **31**, 700.

[3] Lichters, R., Meyer-ter-Vehn, J. and Pukhov, A. 1996 Short-pulse laser harmonics from oscillating plasma surfaces driven at relativistic intensity. *Phys. Plasmas* **3**, 3425.

[4] Grebogi, C., Tripathi, V. K. and Chen, H. H. 1983 Harmonic generation of radiation in steep density profile. *Phys. Fluids* **26**, 1904

[5] Bulanov, S. V., Naumova, N. M. and Pegoraro, F. 1994 Interaction of an ultrashort, relativistically strong laser pulse with an overdense plasma. *Phys. Plasmas* **1**, 745.

[6] Engers, T., Fendel, W., Schüler, H., Schulz, H. and von der Linde, D. 1991 Second-harmonic generation in plasmas produced by femtosecond laser pulses. *Phys. Rev.* A **43**, 4564.

[7] Esarey, E., Ting, A., Sprangle, P., Umstadter, D. and Liu, X. 1993 Nonlinear analysis of relativistic harmonic generation by intense lasers in plasmas. *IEEE Trans. Plasma Sci.* **21**, 95.

[8] Zepf, M. et al. 1998 Role of the plasma scale length in the harmonic generation from solid targets. *Phys. Rev.* E **58**, 5253.

[9] Mori, W. B., Decker, C. D. and Leemans, W. P. 1993 Relativistic harmonic content of nonlinear electromagnetic waves in underdense plasma. *IEEE Trans. Plasma Sci.* **21**, 110.

[10] Wilks, S. C., Kruer, W. L. and Mori, W. B. 1993 Odd harmonic generation of ultra-intense laser pulses reflected from an overdense plasma. *IEEE Trans. Plasma Sci.* **21**, 120.

[11] Rax, J. M. and Fisch, N. J. 1992 Third harmonic generation with ultrahigh intensity laser pulses. *Phys. Rev. Lett.* **69**, 772.

[12] Rax, J. M. and Fisch, N. J. 1993 Phase-matched third harmonic generation in a plasma. *IEEE Trans. Plasma Sci.* **21**, 105.

[13] Liu, C. S. and Tripathi, V. K. 1996 Second-harmonic generation of Raman scattered light in a plasma channel. *Phys. Rev.* E, **54**, 4098.

[14] Sprangle, E. P. and Esarey, E. 1991 Stimulated backscattered harmonic generation from intense laser interaction with beams and plasmas. *Phys. Rev. Lett.* **67**, 2021.

[15] Stamper, J. A., Lehmberg, R. H., Schmitt, A., Herbst, M. J., Young, F. C., Gardner, J. H. and Obenschain, S. P. 1985 *Phys. Fluids* **28**, 2563.

[16] Young, P. E., Baldis, H. A., Johnston, T. W., Kruer, W. L. and Estabrook, K. G. 1989 *Phys. Rev. Lett.* **63**, 2812.

[17] Brandi, H. S., Maia Neto, P. A. and Guerit, E. S. 1996 *Phys. Rev.* E **54**, 1001.

[18] Malka, V. et al. 1997 *Phys. Plasmas.* **4**, 1127.

[19] Meyer, J. and Zhu, Y. 1987 *Phys. Fluids* **30**, 890.

[20] Pukhov, A. 1996 *Phys. Rev. Lett.* **76**, 3975.

https://doi.org/10.1017/S0022377804003319 Published online by Cambridge University Press